Available online at www.sciencedirect.com
ScienceDirect
Ceramics International 34 (2008) 181–188
CERAMICS INTERNATIONAL
www.elsevier.com/locate/ceramint

Non-destructive characterisation of alumina/aluminium titanate composites using a micromechanical model and ultrasonic determinations Part I. Evaluation of the effective elastic constants of aluminium titanate

S. Bueno [a], M.G. Hernández [b], T. Sánchez [b], J.J. Anaya [b], C. Baudín [a,*]

[a] *Instituto de Cerámica y Vidrio, CSIC, Kelsen 5, 28049 Madrid, Spain*
[b] *Instituto de Automática Industrial, CSIC, La Poveda, 28500 Arganda del Rey, Madrid, Spain*

Received 15 May 2006; received in revised form 26 June 2006; accepted 27 September 2006
Available online 22 November 2006

Abstract

A method to evaluate the elastic constants of aluminium titanate in alumina/aluminium titanate composites is described. Results are derived from a three-phase micromechanical model proposed to relate the velocity of propagation of ultrasounds in the materials with their microstructural characteristics and the elastic behaviour of the constituents. Dense and un-cracked alumina and alumina + 10 vol.% aluminium titanate specimens have been fabricated by colloidal processing and the longitudinal and transverse ultrasound velocities have been determined by the ultrasonic jointly pulse-echo and transmission ultrasound-immersion techniques, employing a digital signal processing. In order to assure the adequacy of the proposed method, results for monophase alumina have been compared to those obtained from the resonance frequencies of high density alumina plates tested in flexure and shear. The values of elastic moduli obtained using the two methods were coincident, which assured the validity of the non-destructive proposed method.

Keywords: B. Composites; B. Microstructure; D. Al_2O_3; D. Al_2TiO_5; Ultrasounds

1. Introduction

Improved flaw tolerance of alumina (Al_2O_3)/aluminium titanate (Al_2TiO_5) composites are due to toughening mechanisms originated by residual stresses, developed during cooling from the sintering temperature as a consequence of thermal expansion mismatch between the grains [1–4]. Such stresses might also lead to spontaneous microcracking of the materials during fabrication. Therefore, the suitability of one particular alumina/aluminium titanate composite for an application is determined by the amount of cracks present in the sintered material. In this sense, the possibility of evaluating the extent of cracking in a piece from non-destructive methods is of prime interest.

Ultrasonic velocity in the materials is determined by the elastic properties which, in turn, are determined by the elastic moduli, volume fractions, orientations and distribution of the constituent phases. Therefore, it is possible to use ultrasonic velocity to evaluate the characteristics of the porosity considering it as a constituent void phase. Using a similar approach, and considering microcracks in the material as a void phase with specific shape characteristics, values of the elastic properties of a material, determined by non-destructive methods, could be used to determine extension of cracking once phase composition, density and the elastic properties of the constituent phases are known. In this sense, Young's modulus and Poisson's ratio values of alumina/aluminium titanate composites determined by ultrasonic non-destructive testing (NDT-UT) techniques, together with the phase composition and density of the materials would allow the evaluation of the extension of cracking.

* Corresponding author. Tel.: +34 91 735 58 40; fax: +34 91 735 58 43.
E-mail address: cbaudin@icv.csic.es (C. Baudín).

0272-8842/$32.00
doi:10.1016/j.ceramint.2006.09.006

For such an approach, the elastic constants of aluminium titanate are required. Nevertheless, these constants have not been reported in the literature, probably due to the difficulty of fabrication of dense and un-cracked aluminium titanate materials. In this work, a method to evaluate the effective elastic constants of aluminium titanate in un-cracked alumina/aluminium titanate materials is described. Results are derived from a three-phase micromechanical model proposed to relate the velocity of propagation of ultrasounds in the materials with their microstructural characteristics and the elastic behaviour of the constituents. In the second part of this work [5], the same micromechanical model will be applied to determine the extension of cracking in alumina/aluminium titanate composites using the previously obtained values for the elastic constants of aluminium titanate.

2. Three-phase micromechanical model

Several models have been implemented to predict the elastic modulus of multiphase materials [6]. The two simplest models, by Reuss and Voight, consider a biphasic composite formed by alternating layers of the constituent phases and establish the upper and lower bounds for the Young's modulus of composites formed by random distributions of the second phase. These bounds could be tightened by adjusting the values using empirical constants. Hashin and Shtrikman [7], considering arbitrary second phase geometry in quasi-homogeneous and quasi-isotropic materials, found still more stringent upper and lower bounds. Nevertheless, in general these models have limited success to analyse the effect of porosity. In fact, some models postulate the inclusions to be more rigid than the matrix, whereas, in other cases, the consideration of porosity as a low modulus phase results in the modulus of the composite being equal to that of the matrix [6].

In this work, a three-phase model, previously developed [8] and successfully applied for cement-based materials [9], is used to analyse the elastic behaviour of alumina/aluminium titanate composites with porosity. The formulation of the model is based on average field theory of Mori and Tanaka [10] and Eshelby's [11] equivalent inclusion principle. In the model proposed here, the relationships between the elastic properties of the composite, its density and the transverse and longitudinal ultrasonic wave's velocities are established by means of the micromechanics theory. The composite material is considered to be constituted by a solid matrix (dense alumina), and two types of inclusions: aluminium titanate grains free of cracks (t) and pores (p). For such a material, the elastic constant tensor C is described by [8]:

$$C = C^{\mathrm{m}} + v^{\mathrm{p}}(C^{\mathrm{pm}})\langle T^{\mathrm{p}}\rangle[v^{\mathrm{m}}I + v^{\mathrm{p}}\langle T^{\mathrm{p}}\rangle + v_t\langle T^{\mathrm{t}}\rangle]^{-1} + v^{\mathrm{t}}(C^{\mathrm{tm}}) \times \langle T^{\mathrm{t}}\rangle[v^{\mathrm{m}}I + v^{\mathrm{p}}\langle T^{\mathrm{p}}\rangle + v_t\langle T^{\mathrm{t}}\rangle]^{-1} \quad (1)$$

where

$$C^{\mathrm{pm}} = C^{\mathrm{p}} - C^{\mathrm{m}} \quad \text{and} \quad C^{\mathrm{tm}} = C^{\mathrm{t}} - C^{\mathrm{m}} \quad (2)$$

C^{m}, C^{p} and C^{t}, and v^{m}, v^{p} and v^{t} are the elastic constant tensors and the volume fractions of the matrix (m) and the inclusions (p and t), respectively. T^{p} and T^{t} represent the Wu's tensors [13] in global coordinates for inclusions p and t and I is the symmetric identity tensor. The fourth range tensor T evaluates the geometry, distribution and orientation of the inclusions and the brackets denote the average over all possible orientations.

In order to reduce the elastic tensor C to two independent elastic constants, elastic isotropy of the constituent phases has to be assumed, which is not exact for alumina [14] and is probably not true for aluminium titanate. Even though no elastic data have been reported for this compound, its extreme anisotropy in thermal expansion ($\alpha_{\mathrm{a25-1000\,^\circ C}} = 10.9 \times 10^{-6}\,^\circ\mathrm{C}^{-1}$, $\alpha_{\mathrm{b25-1000\,^\circ C}} = 20.5 \times 10^{-6}\,^\circ\mathrm{C}^{-1}$, $\alpha_{\mathrm{c25-1000\,^\circ C}} = -2.7 \times 10^{-6}\,^\circ\mathrm{C}^{-1}$ [15]) would allow to infer also elastic anisotropy. Nevertheless, although each alumina or aluminium titanate grain will present anisotropy, it is assumed that orientation of the particles in the composite is random and, thus, the effective contribution of the elastic behaviours of both phases to that of the material can be taken as isotropic. Consequently, the term $C^{\mathrm{tm}}\langle T^{\mathrm{t}}\rangle$ in Eq. (1) is an isotropic tensor [16]. Therefore,

$$C_{11} = C_{11}^{\mathrm{m}} - \frac{v^{\mathrm{p}}(C_{11}^{\mathrm{m}} - (4/3)C_{44}^{\mathrm{m}})\langle T^{\mathrm{p}}\rangle}{1 - v^{\mathrm{p}} - v^{\mathrm{t}} + v^{\mathrm{p}}\langle T^{\mathrm{p}}\rangle + v^{\mathrm{t}}\langle T^{\mathrm{t}}\rangle} + \frac{v^{\mathrm{t}}(C_{11}^{\mathrm{tm}} - (4/3)C_{44}^{\mathrm{tm}})\langle T^{\mathrm{t}}\rangle}{1 - v^{\mathrm{p}} - v^{\mathrm{t}} + v^{\mathrm{p}}\langle T^{\mathrm{p}}\rangle + v^{\mathrm{t}}\langle T^{\mathrm{t}}\rangle} + \frac{(8/3)v^{\mathrm{p}}(-C_{44}^{\mathrm{m}})\langle T_{1212}^{\mathrm{p}}\rangle + (8/3)v^{\mathrm{t}}(C_{44}^{\mathrm{t}} - C_{44}^{\mathrm{m}})\langle T_{1212}^{\mathrm{t}}\rangle}{1 - v^{\mathrm{p}} - v^{\mathrm{t}} + 2v^{\mathrm{p}}\langle T_{1212}^{\mathrm{t}}\rangle + 2v^{\mathrm{t}}\langle T_{1212}^{\mathrm{t}}\rangle} \quad (3)$$

$$C_{44} = C_{44}^{\mathrm{m}} + \frac{v^{\mathrm{p}}(-C_{44}^{\mathrm{m}})2\cdot\langle T_{1212}^{\mathrm{p}}\rangle + v^{\mathrm{t}}(C_{44}^{\mathrm{t}} - C_{44}^{\mathrm{m}})2\cdot\langle T_{1212}^{\mathrm{t}}\rangle}{1 - v^{\mathrm{p}} - v^{\mathrm{t}} + 2v^{\mathrm{p}}\langle T_{1212}^{\mathrm{p}}\rangle + 2v^{\mathrm{t}}\langle T_{1212}^{\mathrm{t}}\rangle} \quad (4)$$

where

$$C_{11}^{\mathrm{tm}} = \bar{C}_{11}^{\mathrm{t}} - C_{11}^{\mathrm{m}}, \qquad C_{44}^{\mathrm{tm}} = \bar{C}_{44}^{\mathrm{t}} - C_{44}^{\mathrm{m}} \quad (5)$$

$$\langle T^{\mathrm{p}}\rangle = \langle T_{1111}^{\mathrm{p}}\rangle + 2\langle T_{1122}^{\mathrm{p}}\rangle, \qquad \langle T^{\mathrm{t}}\rangle = \langle T_{1111}^{\mathrm{t}}\rangle + 2\langle T_{1122}^{\mathrm{t}}\rangle \quad (6)$$

C_{ij} are the independent components of the elastic tensor in reduced notation; T, m, t, and p have the same meaning as before, and $\bar{C}^{\mathrm{t}}$ are the effective elastic constants of aluminium titanate in the composite material.

The relation between the volume fractions of the matrix and the inclusions, v^{p} (pores) and v^{t} (aluminium titanate) is given by

$$v^{\mathrm{m}} = 1 - v^{\mathrm{p}} - v^{\mathrm{t}} \quad (7)$$

The independent elastic constants are related to the longitudinal and transverse propagation velocities of ultrasounds (V_{L} and V_{T}, respectively) by

$$V_{\mathrm{L}} = \sqrt{\frac{C_{11}}{\rho}}, \qquad V_{\mathrm{T}} = \sqrt{\frac{C_{44}}{\rho}} \quad (8)$$

The relation between C_{11}, C_{44} and the Young's modulus, E, and the Poisson's ratio μ are:

$$E = \frac{C_{44}(3C_{11} - 4C_{44})}{C_{11} - C_{44}}, \qquad \mu = \left(\frac{E}{2C_{44} - 1}\right) \tag{9}$$

If ρ^m and ρ^t are the density of the matrix and the aluminium titanate, the density of the composite material, ρ, is given by

$$\rho = (1 - v^p - v^t)\rho^m + v^t\rho^t \tag{10}$$

In order to apply the model, a reduction of the number of variables is necessary. This can be achieved by analysing the shape and distribution of the inclusions, pores and aluminium titanate particles. Also, accurate determinations of the density of the composite and the longitudinal and transverse ultrasonic velocities are needed. A precise experimental method is required to determine the high velocities of the ultrasonic waves through the studied materials in order to minimise errors. Once these requirements are fulfilled, the above expressions allow evaluating the elastic constants of alumina and aluminium titanate, C^m and $\bar{C}^t$. Due to the complexity of the model numerical methods are used for the evaluation. The algorithms are based on a combination of bisection, secant and quadratic interpolation methods.

3. Experimental

3.1. Material processing

Alumina (Al_2O_3) monophase materials and alumina + 10 - vol.% aluminium titanate (Al_2TiO_5) composites were obtained using alumina with and without MgO (Condea HPA-0.5 w/MgO and Condea HPA05, USA, respectively) and titania, TiO_2 (Merck, 808, Germany) as starting powders. In previous works [4,17], the processing conditions to fabricate dense and completely reacted alumina/aluminium titanate composites with a homogeneous dispersion of the second phase, using colloidal filtration techniques, were established. Monophase alumina blocks (90 mm × 50 mm × 12 mm) made of MgO-doped alumina were prepared by attrition milling of the alumina powders in ethanol, drying, isostatic pressing (200 MPa) and sintering at 1550 °C for 1 h in order to achieve density higher than 99% of the theoretical. For the monophase alumina and alumina–10 vol.% aluminium titanate composite obtained by colloidal filtration, stable suspensions of a mixture of undoped alumina and titania to a solid loading of 80 wt.% were prepared by ball milling and green compacts of 70 mm × 70 mm × 12 mm were made by colloidal filtration on plaster of Paris moulds. The sintering was performed using heating and cooling rates of 2 °C min^{-1} and a dwell of 4 h at 1200 °C during the heating, and a high temperature dwell of 2 h at 1450 °C. In the following, for easier identification, the sintered samples have been labelled using A_{HD} (HD, high density) for the monophase alumina material sintered at 1550 °C for 1 h, and A and A-10AT for the monophase and composite materials processed by colloidal filtration (1450 °C for 2 h).

3.2. Material characterisation

Densities of the sintered compacts were determined by Archimedes's method in water (European Standard EN 1389:2003) and relative densities were calculated from these values and those of theoretical densities calculated taking values of 3.99 g cm^{-3} for alumina (ASTM File 42-1468) and 3.70 g cm^{-3} for aluminium titanate (ASTM File 26-0040).

Microstructural characterisation was performed by field emission scanning electron microscopy (FE-SEM, Hitachi, S-4700, Japan) on polished and thermally etched (20 °C below the sintering temperature during 1 min) surfaces.

Pieces of 10 mm × 5 mm × 5 mm cut from the sintered blocks were tested in a differential dilatometer (402 EP, Netzsch, Germany) to obtain the thermal expansion curves on heating and cooling at 5 °C min^{-1}. Three determinations were performed for each material and the curves of the three experiments were found to be practically coincident.

Young's modulus and Poisson's coefficient of high dense alumina (A_{HD}) were calculated from the resonance frequencies (Grindosonic, J.W. Lemmens, Belgium) of plates (30 mm × 30 mm × 4 mm) tested by impact in flexure and shear and the density. Determinations were done on three plates machined from the sintered blocks; results and error are the average and the standard deviation of the three determinations. Young's modulus of the other two materials were determined from the resonance frequency of bars tested in flexure by impact and the densities, using for calculations the value of the Poisson's coefficient obtained for A_{HD}. Samples were machined from the sintered blocks into bars of 4 mm × 3 mm × 50 mm; reported values are the average of five determinations and errors are the standard deviations.

3.3. Ultrasonic determinations

Ultrasonic velocities were determined for the materials obtained by colloidal filtration (A and A-10AT). The green compacts were cut in two equal prism-shaped specimens of approximate dimensions 35 mm × 70 mm × 12 mm and the blocks were machined to have parallel faces in the thickness direction after sintering (thickness ≅ 9.4 mm). Determinations were done by the immersion technique at normal (longitudinal velocity) and oblique angles (transverse velocity) of incidence into the thickness direction. All measurements were done with two transducers of broadband (80%), 5 MHz centre frequency and 10 mm diameter (Krautkramer H5K). Transducers were excited by a spike voltage of about 200 V, the data were obtained in the time domain and the acquired signals were sampled at 100 MHz. In order to determine the time-of-flight of the ultrasonic waves with high precision, the signals were digitally processed to obtain the first crossing by zero, to obtain smaller errors (<10 ns) of relative times.

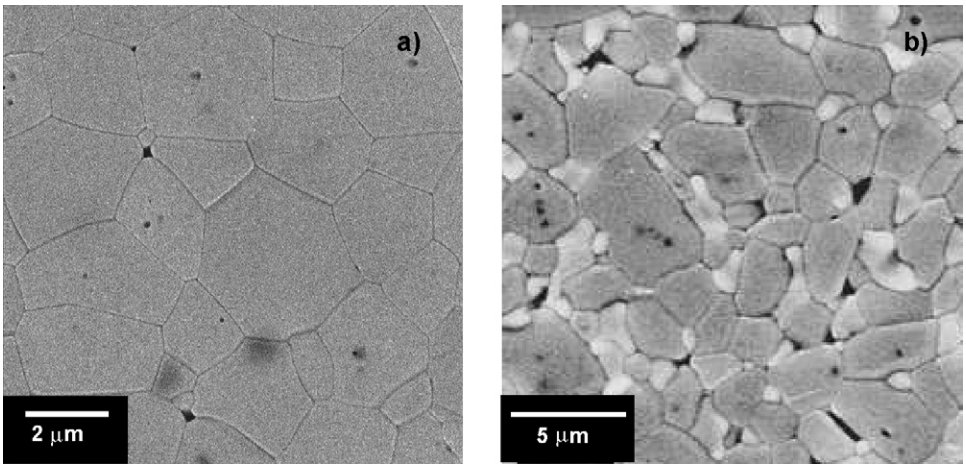

Fig. 1. Scanning electron micrographs of polished and thermally etched surfaces of the studied materials. In the composites, aluminium titanate grains (white) are localised mostly at grain boundaries and triple points in the alumina (grey) matrix: (a) A and (b) A-10AT.

4. Results and discussion

4.1. Microstructure and properties

Characteristic microstructures of the A and A-10AT materials are shown in Fig. 1 and Table 1 lists the relative densities of the studied materials together with the values of the Young's modulus determined from the resonance frequencies. As no open porosity was observed in any of the materials, being porosity formed by small ($\leq$1 μm) closed pores; total porosity can be calculated as the difference between the theoretical density and the experimental density values from Table 1. In the composite, slightly elongated aluminium titanate grains were homogeneously distributed, and no titania was observed at this level (SEM).

For both materials, A and A-10AT, the thermal expansion curves on heating and cooling were coincident (Fig. 2a and b) as occurs in microcrack free ceramics [16–18]. This kind of behaviour is in agreement with the lack of microcracks observed in the microstructures by SEM (Fig. 1).

As discussed in Section 1, some assumptions have to be done in order to simplify the three-phase model developed before application. These assumptions are derived from the observations of the microstructures (Fig. 1) described above. Material A (Fig. 1a) had only two constituents, equidimensional alumina grains and closed pores uniformly distributed in the matrix. Material A-10AT (Fig. 1b) was also constituted by

Table 1
Relative density, ρ, total porosity, P, and Young's modulus determined from the resonance frequency, E, of the samples

	ρ (% of theoretical) (experimental)	P (%) (calculated from ρ)	E (GPa)
A_{HD}	99.6 ± 0.1	0.4	412 ±6
A	97.7 ± 0.2	2.3	387 ± 5
A-10AT	97.9 ± 0.2	2.1	355 ± 4

The high density monophase alumina (A_{HD}) was tested in flexure and shear and the determined Poisson's coefficient was 0.22 ± 0.02.

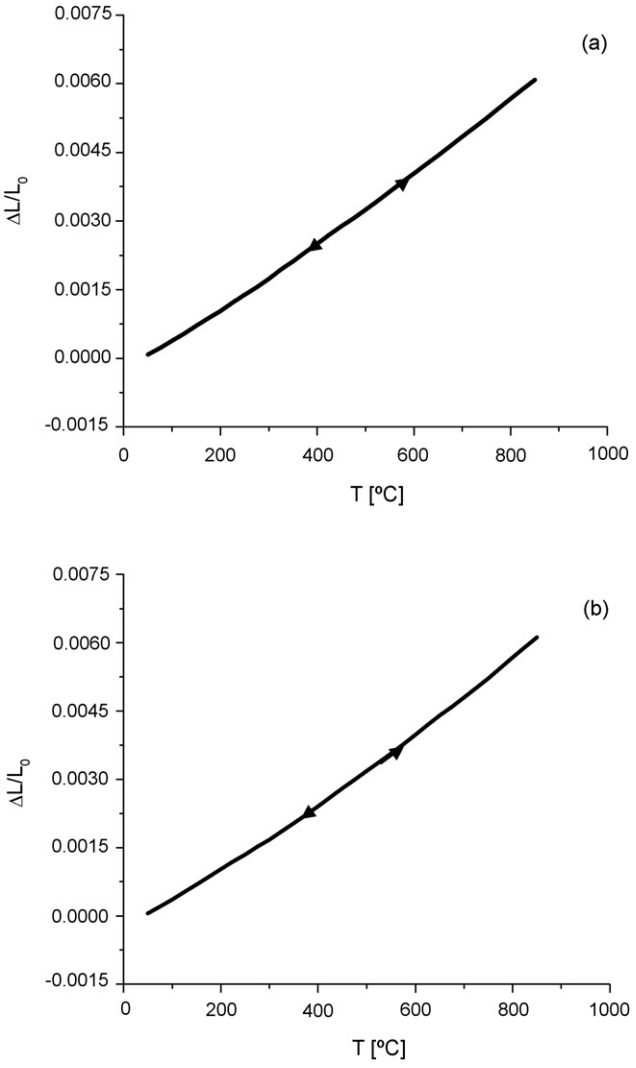

Fig. 2. Thermal expansion curves of the studied materials on heating and cooling at 5 °C min^{-1}. Reversibility was obtained in all cases: (a) A and (b) A-10AT.

equidimensional alumina grains and closed pores. Aluminium titanate grains, slightly elongated, were randomly and homogeneously distributed through the matrix. Therefore, both materials can be considered statistically isotropic in average. On the other hand, the closed porosity can be well described as spherical whereas the aluminium titanate grains can be described as ellipsoids.

4.2. Ultrasonic determinations

4.2.1. Longitudinal velocity

The experimental set-up for the determination of the longitudinal velocity is schematically illustrated in Fig. 3a. The ultrasonic wave at right angle to the sample was first transmitted and then successively reflected by the two faces of the sample. In Fig. 3a, the time-of-flight t_1 is the propagation time to the pulse transmitted through the specimen, and t_2, t_3, and t_4 are times of flight of the three first back-wall echoes. Measuring the average delay time between two consecutive echoes $\Delta t = t_n - t_{n-1}$ and knowing the width, s, of the sample the longitudinal velocity was calculated as $V_L = 2s/\Delta t$.

Fig. 3b shows the received signal when the wave stroke perpendicularly sample A. The obtained values of the longitudinal velocity for both samples are: V_L (A) = 10,740 m s^{-1} and V_L (A-10AT) = 10,442 m s^{-1}, with an error, calculated from the precision of the time-of-flight, inferior to 1%.

4.2.2. Transverse velocity

When an ultrasonic wave transmitted by a fluid, water in the experimental set-up used in this work, strikes obliquely a solid body, at an angle of incidence α to the perpendicular, the incident wave is divided into a longitudinal and a transverse waves. When these two waves reach the opposite interface between the solid material and the fluid, two beams of longitudinal waves are generated; if the body has parallel surfaces these longitudinal waves are parallel. The experimental set-up is illustrated in Fig. 4a, where only the transmitted waves are shown; the reflected waves have been omitted for simplicity. For the determination of the ultrasound velocity (V_T), the general formula has been used [12]:

$$V_T = \frac{d}{t - t_w + (d/V_w)} \tag{11}$$

where d is the path length of the wave in the specimen, t the time of transmission when the sample is located between both

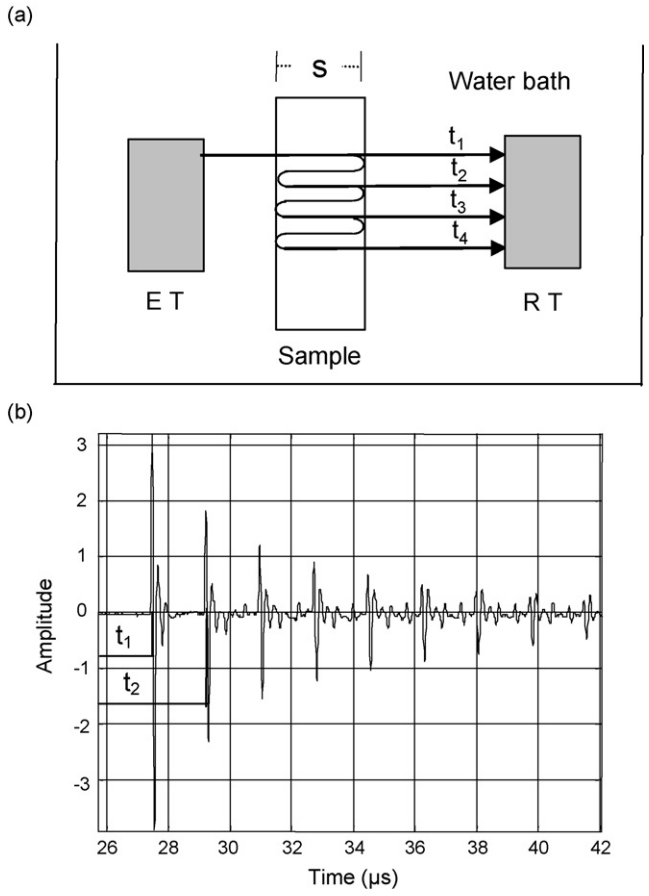

Fig. 3. (a) Signal paths of ultrasound wave in the immersion experiment for longitudinal velocity measurements. (b) Multiple echoes in the longitudinal wave transmitted. Perpendicular incidence.

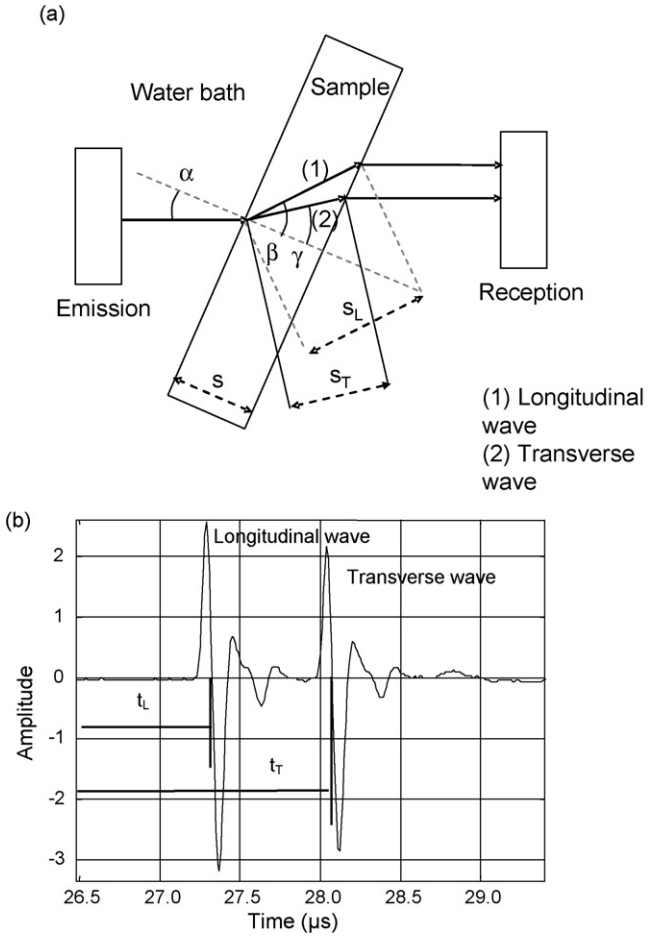

Fig. 4. (a) Signal paths of ultrasound waves in the immersion experiment for transverse velocity measurements. (b) Transverse and longitudinal waves transmitted. Oblique incidence.

transducers, t_w the time taken for the wave travelling through water between the transducers, and V_w is the velocity in water.

The specimen was turned so that the receiver transducer received simultaneously the longitudinal and the transverse waves with similar amplitude (Fig. 4b). Applying the laws of Snell for both types of transmitted waves and according to Fig. 4a, the following fourth order system of equations is obtained (12):

$$V_L = \frac{s_L}{t_L - t_w + (s_L/V_w)}, \qquad V_T = \frac{s_T}{t_T - t_w + (s_T/V_w)},$$
$$\frac{\sin\beta}{\sin\gamma} = \frac{V_L}{V_T}; \quad s_L = \frac{s}{\cos\beta}; \qquad s_T = \frac{s}{\cos\gamma} \tag{12}$$

where V_L, s_L, t_L, γ, are the velocity, the crossed length, the time-of-flight and the angle of transmission of the longitudinal wave to travel (through the sample and water), respectively, V_T, s_T, t_T, β are the corresponding values for the transverse wave and V_w the velocity of sound in water.

Because the values t_L, t_T and t_w are obtained experimentally from the transmitted signal, it is possible to calculate the value of transverse velocity V_T, with no need of knowing the angle of incidence. The values obtained for the transverse velocity were V_T(A) = 6434 m s^{-1} and V_T(A-10AT) = 6190 m s^{-1}.

4.3. Evaluation of the elastic constants of alumina

In Fig. 5, the theoretical relationships between the ultrasonic velocities and the Young's modulus of the fully dense matrix, E^m, of alumina materials with the same microstructural characteristics as the one characterised here, A, are plotted for five different values of the Poisson's coefficient. Longitudinal and transverse velocities were calculated applying Eqs. (3)–(10) (ρ value for A in Table 1) for varying values of Young's modulus and Poisson's ratio of matrix, E^m [400, 420] and μ^m [0.210, 0.230]. The corresponding variation ranges for elastic constant tensors are $C_{11}^m = [450, 490]$ and $C_{44}^m = [162, 174]$. Isotropy and uniform distribution of spherical pores, as discussed above, was assumed. From these plots, both velocities increase with Young's modulus whereas and increase in Poisson's ratio causes an increment of the longitudinal velocity (Fig. 5a) and a decrease of the transverse velocity (Fig. 5b).

In Fig. 5, the lines parallel to the X-axis corresponding to the experimental values of the longitudinal and transverse velocities give straight lines defined by the possible pairs (E^m, μ^m) for each velocity. The intersection of these lines (Fig. 6) gives the values of the Young's modulus (410 GPa) and the Poisson's ratio (0.223) that would correspond to the fully dense alumina matrix of material A according to the applied model. The corresponding values for elastic constant tensors are $C_{11}^m = 470$ and $C_{44}^m = 168$. The obtained values of Young's modulus and Poisson ratio are similar to those determined experimentally for the high density alumina (A_{HD}, Table 1). This fact supports the adequacy of the proposed model to evaluate the elastic constants of the alumina matrix in the composites.

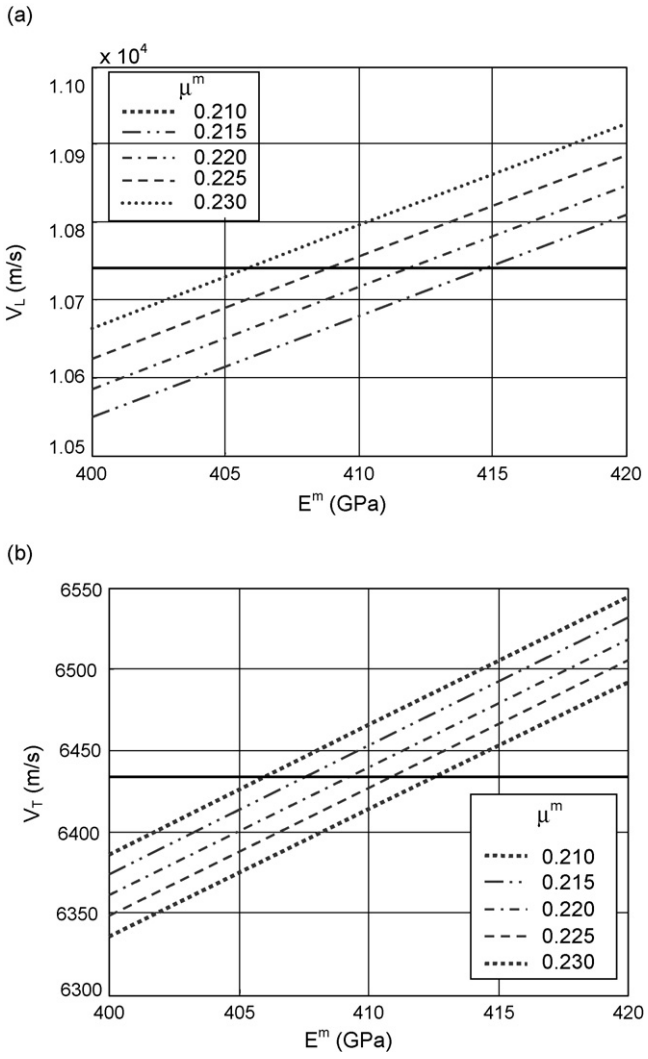

Fig. 5. Theoretical relationships between the ultrasound velocities and the elastic constants for the dense alumina matrix derived from the model (dotted lines). The continuous horizontal lines represent the experimental measurements: (a) longitudinal velocity and (b) transverse velocity.

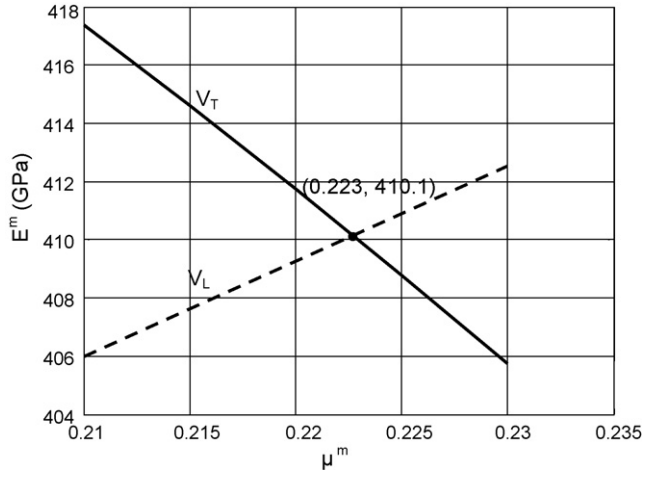

Fig. 6. Estimation of the elastic constants of the alumina matrix from the experimental values of the longitudinal and transverse ultrasound velocities and the relationships in Fig. 5.

4.4. Evaluation of the effective Young's modulus of aluminium titanate

In order to evaluate the effective Young's modulus of aluminium titanate in the composite material, A-10AT, similar assumptions of isotropy and uniform distribution of spherical pores as for the monophase alumina, A, were done. In this case, the solid phase was constituted by alumina (90 vol.%) and aluminium titanate (10 vol.%). The slightly elongated shape of the aluminium titanate grains was modelled by an extended prolate ellipsoid with shape factor, defined as the ratio between the major and minor axes, of 1.4. The same graphical procedure as for the monophase alumina was utilized once Eqs. (3)–(10) were solved for E^t [100, 180] and μ^t [0.28, 0.36] using the value of Young's modulus previously determined for the alumina matrix (410 GPa) and the density of material A-10AT from Table 1. The corresponding ranges for the elastic constants of aluminium titanate were $C_{11}^t = [128, 303]$ and $C_{44}^t = [37, 70]$. In Figs. 7 and 8 the graphical procedure is shown. Values of

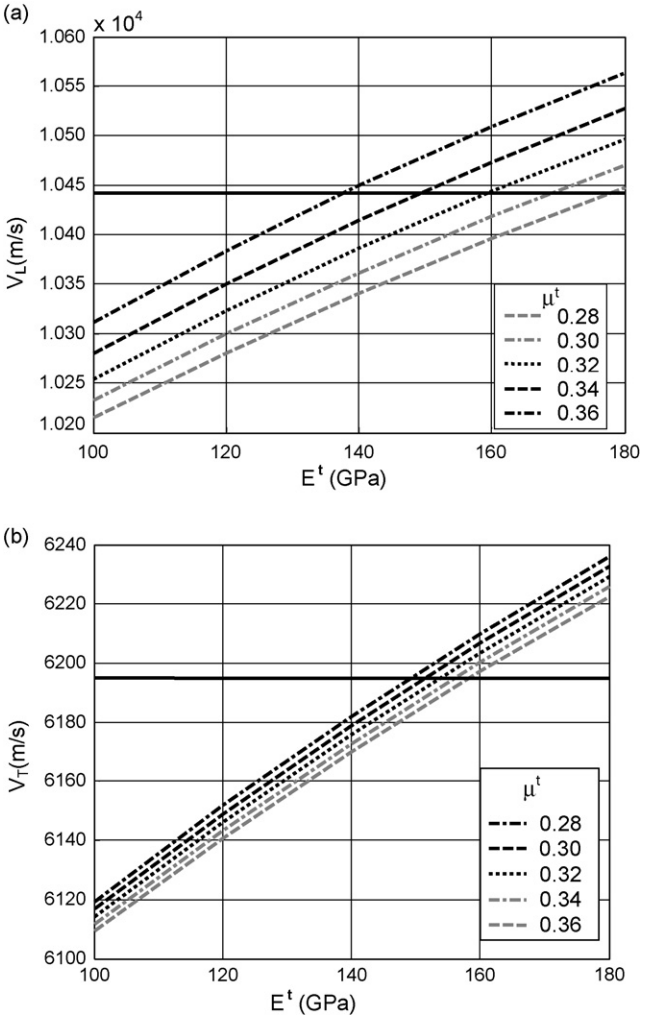

Fig. 7. Theoretical relationships between the longitudinal and transverse velocities in the A-10AT composite versus elastic constants of aluminium titanate derived from the model (dotted). The continuous horizontal lines represent the experimental measurements: (a) longitudinal velocity and (b) transverse velocity.

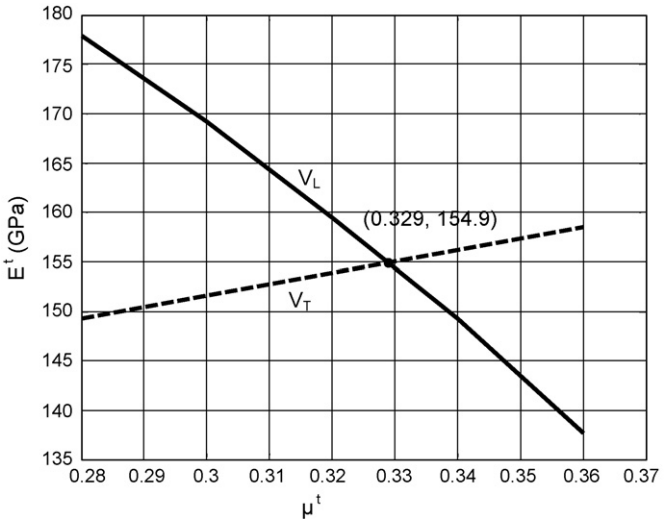

Fig. 8. Estimation of the effective elastic constants of the aluminium titanate particles from the experimental values of the longitudinal and transverse ultrasound velocities and the relationships in Fig. 7.

154.9 GPa and 0.329 were found for the effective Young's modulus, E^t, and Poisson's ratio, μ^t, respectively, of aluminium titanate in the studied material (Fig. 8). The corresponding values for the elastic constants were $C_{11}^t = 239$ and $C_{44}^t = 58$.

Even tough, as discussed in the introduction, Young's modulus of monophase crack free aluminium titanate materials has not been experimentally determined, some comparisons with values for other pseudobrookites can be done to analyse the adequacy of the value obtained here. This value is slightly lower than that obtained for crack free Fe_2TiO_5 (≅172 GPa), for which the Young's modulus of the cracked material (≅40 GPa) was slightly higher than that of cracked Al_2TiO_5 (≅25 GPa) [19], and significantly lower than that reported for $MgTi_2O_5$ (≅240 GPa), for which Young's modulus of the cracked material (≅125 GPa) was significantly higher than that of cracked Al_2TiO_5 [18]. Then, it is reasonable to consider the obtained Young's modulus value of aluminium titanate as valid. Even tough the aspect of the microstructures (Fig. 1) together with the characteristics of the thermal expansion curves (Fig. 2), indicate that microcracking is not significant in the studied composite, some aluminium titanate grains, larger than the critical one (≈2.2 μm [3]), might present internal cracking due to its thermal expansion anisotropy. Therefore, the values of the elastic constants determined in this work should be considered as effective and suitable to analyse the behaviour of other alumina/aluminium titanate composite materials with similar aluminium titanate grain sizes. In order to check this possibility, the three-phase model was applied to calculate the Young's modulus values for the dense and un-cracked materials from Ref. [3]. Table 2 shows the comparison between the experimental values and those calculated from the volume fractions of the components and the elastic constants for the dense components, alumina and aluminium titanate, obtained in this work. The complete agreement observed demonstrate the validity of the method and the elastic constants evaluated here.

Table 2
Relative density, ρ, total porosity, P, and Young's modulus determined from the resonance frequency, E_e, and three-phase model prediction, E_p, of materials from [3]

	ρ (% of theoretical) (experimental)	P (%) (calculated from ρ)	E_e (GPa) (experimental)	E_p (GPa) (prediction)
A	98.7 ± 0.5	1.3	405 ± 2	401 ± 4
A-5T	98.4 ± 0.2	1.6	383 ± 5	384 ± 4
A-10AT	98.5 ± 0.2	1.5	375 ± 5	371 ± 5

In a similar way, this methodology could be used to evaluate the porosity and/or the presence of microcracks in materials, from the ultrasonic velocities and the volume fractions of the constituents. In part II [5] of this work, the suitability of the methodology to evaluate the appearance of microcracks in alumina/aluminium titanate composites is analysed.

5. Conclusions

It is possible to evaluate the effective elastic parameters, Young's modulus and Posisson's coefficient, of second phases from the longitudinal and transverse ultrasonic velocities by using a micromechanical model of three phases once the characteristics of the matrix are known. This methodology has been applied to evaluate the properties of aluminium titanate in alumina/aluminium titanate composites. To determine with high accuracy the ultrasonic velocities the jointly pulse-echo and transmission ultrasound-immersion techniques, employing a digital signal processing, could be used. The immersion technique gives constant coupling without wear and also allows changing easily the incidence angle to obtain either longitudinal o transverse waves. This methodology would make possible to create a simple instrument of semiautomatic measurement for a very precise determination of the elastic constants of the multiphase materials.

Acknowledgements

The financial support of Spanish Ministry of Science and Technology (Project DPI 2003-08628-C03-00) and the Projects CICYT MAT2003-00836 and CAM GRMAT0707-2004 is acknowledged. M.G. Hernández is supported by a postdoctoral CSIC-I3P contract granted by the European Social Fund. S. Bueno acknowledges the financial support of the Grant CSIC I3P-BPD2001-1 (Spain).

References

[1] N.P. Padture, S.J. Bennison, H.M. Chan, Flaw-tolerance and crack-resistance properties of alumina–aluminium titanate composites with tailored microstructure, J. Am. Ceram. Soc. 76 (1993) 2312–2320.
[2] N.P. Padture, J.L. Runyan, S.J. Bennison, L.M. Braun, B.R. Lawn, Model for toughness curves in two-phase ceramics. II. Microstructural variables, J. Am. Ceram. Soc. 76 (1993) 2241–2247.
[3] R. Uribe, C. Baudín, Influence of a dispersión of aluminum titanate particles of controlled size on the thermal shock resistance of alumina, J. Am. Ceram. Soc. 86 (2003) 846–850.
[4] S. Bueno, R. Moreno, C. Baudín, Design and processing of Al_2O_3–Al_2TiO_5 layered structures, J. Eur. Ceram. Soc. 25 (2005) 847–856.
[5] M.G. Hernández, S. Bueno, T. Sa?nchez, J.J. Anaya, C. Baudı?n, Non-destructive characterisation of alumina/aluminium titanate composites using a micromechanical model and ultrasonic determinations, Ceram. Int. 34 (2008) 189–195.
[6] P.K. Mehta, P.J.M. Monteiro, Concrete Structure. Properties and Materials, 2nd ed., Prentice Hall Inc., Englewood Cliffs, NJ, 1993.
[7] Z. Hashin, S. Shtrikman, A variational approach the theory of the elastic behaviour of multiphase materials, Mech. Phys. Solids 11 (1963) 127–140.
[8] M.G. Hernández, J.J. Anaya, L.G. Ullate, A. Ibañez, Formulation of a new micromechanic model of three phases for ultrasonic characterization of cement-based materials, Cement Concrete Res. 36 (2006) 609–616.
[9] M.G. Hernández, J.J. Anaya, L.G. Ullate, M. Cegarra, T. Sánchez, Application of a micromechanical model of tree phases to estimating the porosity of mortar by ultrasound, Cement Concrete Res. 36 (2006) 617–624.
[10] T. Mori, K. Tanaka, Average stress in matrix and average elastic energy of materials with misfitting inclusions, Acta Metall. 21 (1973) 571–574.
[11] J.D. Eshelby, The determination of the elastic field of an ellipsoidal inclusion and related problems, Proc. R. Soc. London A 241 (1957) 376–396.
[12] K. David, S. Michael, S. Hughes, Simultaneous ultrasonic velocity and sample thickness measurement and application in composites, J. Acoust. Soc. Am. 92 (1992) 669–675.
[13] T.T. Wu, The effect on inclusion shape on the elastic moduli of a two place material, Int. J. Solids Struct. 2 (1–8) (1966).
[14] E.C. Dickey, C.S. Frazer, T.R. Watkins, C.R. Hubbard, Residual stresses in high-temperature ceramic eutectics, J. Eur. Ceram. Soc. 19 (1999) 2503–2509.
[15] D. Taylor, Thermal expansion data. XI. Complex oxides, A_2BO_5, and the garnets, Brit. Ceram. Trans. J. 86 (1987) 1–6.
[16] J.E. Vourinem, Elastic constant of an aluminium–alumina unidirectional composite, J. Acoust. Soc. Am. 108 (2000) 574–579.
[17] S. Bueno, R. Moreno, C. Baudín, Reaction sintered Al_2O_3/Al_2TiO_5 microcrack-free composites obtained by colloidal filtration, J. Eur. Ceram. Soc. 24 (2004) 2785–2791.
[18] J.A. Kuszyk, R.C. Bradt, Influence of grain size on effects of thermal expansion anisotropy in $MgTi_2O_5$, J. Am. Ceram. Soc. 56 (1973) 420–423.
[19] J.J. Cleveland, R.C. Bradt, Grain size/microcracking relations for pseudobrookite oxides, J. Am. Ceram. Soc. 61 (1978) 478–481.